J Solid State Electrochem (2009) 13:1003–1014
DOI 10.1007/s10008-008-0697-x

REVIEW

Investigations on some electrochemical aspects of lithium-ion ionic liquid/gel polymer battery systems

A. Guerfi · M. Dontigny · Y. Kobayashi · A. Vijh · K. Zaghib

Received: 26 June 2008 / Revised: 10 September 2008 / Accepted: 29 September 2008 / Published online: 17 October 2008

Abstract Electrochemical and interfacial characteristics of Li-ion battery system based on $LiFePO_4$ cathode and graphite anode with ionic liquid (IL) electrolytes have been investigated, both with and without addition of a small amount of polymer to the electrolyte. The IL electrolyte consisted of bis(fluorosulfonyl)imide (FSI) as anion and 1-ethyl-3-methyleimidazolium (EMI) or *N*-methyl-*N*-propylpyrrolidinium (Py13) as cation, and operated at ambient temperature. We reported previously that the SEI formation with IL was stabilized in the graphite anode at 80% coulombic efficiency (CE) in the first cycle, when FSI anion is used. In this work, we extend the study to the $LiFePO_4$ cathode material. Gel polymer with IL is one part of this study. The stepwise impedance spectroscopy was used to characterize the Li/IL-Gel polymer/$LiFePO_4$ at different states of charge. This technique revealed that the interface resistance was stabilized when the cathode is at 70% DoD (Depth of Discharge). The diffusion resistance is higher at the two extremes of discharge when monophase $LiFePO_4$ state (0%DoD and 100%DoD) obtains. When polymer is added to the IL, interface resistance is improved with 1 wt.% but results with IL alone are not improved for the case of 5 wt.% polymer added. Good cycling life stability was obtained with Li/IL-FSI/$LiFePO_4$ cells, with or without polymer. The first evaluation of the Li-ion cell, $LiFePO_4$/IL-FSI-(5 wt.%) gel polymer/graphite, has shown low first CE at 68.4% but it recovers in the third cycle, to 96.5%. Some capacity fade was noticed after 30 cycles. The rate capability of the Li-ion cell shows a stable capacity until 2 C discharge rate.

Dedicated to Professor J.O' M. Bockris, whose contributions to electrochemistry are inestimable and indelible, on his eighty-fifth birthday.

A. Guerfi (✉) · M. Dontigny · Y. Kobayashi · A. Vijh · K. Zaghib
Institut de Recherche d'Hydro-Québec,
Varennes, QC, Canada
e-mail: guerfi@ireq.ca

Y. Kobayashi
Central Research Institute of electric Power Industry,
2-11-1, Iwado Kita, Komae-shi,
Tokyo 201-8511, Japan

Introduction

Lithium-ion batteries play a pivotal role in modern society since they are the power sources of choice in a variety of electronic devices: portable computers, cameras, personal digital assistants, medical instrumentation and hand-held internet devices, etc. A recent focus is the possible penetration of these batteries in hybrid electric vehicles (HEV) and plug-in HEV (PHV) [1–4]; however, this cannot be achieved before substantial further improvements such as low cost, safety, high-power capability and long calendar life [5, 6]. Although high-power capability can be obtained by combining these batteries with supercapacitors and low cost by new approaches of product engineering, safety is still one of the issues for advanced applications of Li-ion batteries. We think that, safety and long calendar life can only be realized by fundamental changes in the chemistry of the battery system. Of all these factors, the most crucial is the safety. Our recent and current work, as well as that of some other investigators, is aimed at creating lithium-ion-battery chemistries that contribute to better safety. Our work focuses on the use of ionic liquids or ionic liquid-polymer electrolytes, to achieve safety and longer life for the lithium-ion batteries.

Traditionally, ionic liquids were constituted by "molten salts" which become liquids only at high temperatures. However, the evolution in this field in the last couple of decades or so has produced a number of "room temperature" ionic liquids (RTIL) which melt at ordinary temperatures and have many interesting properties (Table 1); these electrolytes are constituted by organic ring (aromatic or hetercyclic) cations and inorganic anions.

Ionic liquids show an inverse relationship between their viscosity and conductivity; hence one should aim to choose ionic liquids with low viscosities in order to have batteries with low internal resistance and high reaction rates.

It is important to emphasize that the inverse correlation between conductivity and viscosity is not just an empirical observation but arises for all liquids including liquid gases, liquid metals, organic liquids, ionic liquids and molten salts, for fundamental theoretical reasons. First, it should be noted that the Arrhenius type of activation energies for viscous flow, E_η, self-diffusion of cations E_{D+}, and anions E_{D-}, all reveal practically the same value in these liquid systems [7, 8]:

$$E_\eta \approx E_{D+} \approx E_{D-} \approx 3.7RT_m \quad (1)$$

where R is the gas constant and T_m is melting point, in degrees Kelvin, of these liquids; strictly speaking, the ordinary connotation of melting point applies to molten salts and metals, since most gases, organic liquids and ionic liquids are not solids at room temperature; in other words T_m is the temperature of phase change, in degrees Kelvin, that gives rise to the liquid state. Theoretically, Eq. (1) can be interpreted by deducing the heat of activation for transport in liquids in terms of work of hole formation in the liquid, as done by Bockris and coworkers [7–9], following original formulation of Fürth [10]. Thus, one must seek for a battery a liquid (ionic or otherwise) with the lowest melting point, in order to attain the highest conductivity.

Most popular ILs consist of quaternary ammonium cations such as imidazolium, pyridinium, pyrrolidinium, sulfonium, ammonium and phosphonium with anions having low Lewis basicities; such as BF_4^-, PF_6^-, $CF_3SO_3^-$, and $(CF_3SO_2)_2N^-$. The quaternary ammonium ions produce a low melting point, compared to the inorganic salts of the same anions, which approaches the room temperature. These RTILs are known as green solvents due to their advantages of non-flammability, high electrochemical stability, low vapor pressure and high conductivity [11, 12]. From the point of view of their use in lithium-ion batteries, their most outstanding features are no vapor pressure, thence, enhanced safety, good electrochemical stability, excellent solvent characteristics and a large voltage window (>5 V vs. Li) for many ILs. Other aspect of these ILs is their high thermal stability, many of them showing decomposition temperatures above 300 °C: this allows one to operate batteries at high temperatures and extends the safety range of the battery, particularly when used in an electric vehicle. Owing to these advantages of these electrolytes, they find much interest in batteries and capacitors [13–15]. Since these ILs have more stable cations, which make the electrochemical stability window wider and allow a larger variety of cathodes to be used, including 5.0 V cathodes. Most of the work on the cathode materials has been explored on $LiCoO_2$ with different ILs [16–20].

Other ILs, different from aromatic rings and hetero cycles, and based on aliphatic quaternary ammonium salts with methoxyethyl groups on the nitrogen atom combined with anions like (BF_4^-) or [$TFSI^-$:$CF_3SO_2)_2N^-$] giving DME-BF_4 and DEME-TFSI, have been also extensively studied [21–25]. Such ILs also have other advantages compared to imidazolium, pyridinium, pyrrolidinium, sulfonium, e.g., large potential window (6.0 V) which makes them very attractive for batteries and particularly capacitors [26–28]. On the anode side the problem of IL is more important due the to the SEI layer formation on some materials such as carbon and anode alloys materials with high capacity. Many researchers study the electrochemical intercalation in graphite anodes in EMI based IL, because of its low viscosity and high conductivity. However, some decomposition of the cations occurs and prevents the intercalation process. Some organic solvents can suppress the reduction of EMI; 5 wt.% VC was added to the EMI-TFSI by the Novak group [29, 30] and they obtained high reversible capacity of the anode with 350 mAh/g. Sato et al. demonstrated the cyclability of Li-ion (graphite/$LiCoO_2$) [31] in DEME-FSI with 10 wt.% VC additive. Other work has examined high capacity silicon anodes using methyl-1-propylperidinium-TFSI known as PP13-TFSI silicon [32], and, SiO_x mixed with carbon using Py13 based IL [33].

Recently Aurbach et al. found that intercalation in the graphite anode occurs simultaneously with IL-cations and Li^+ cations at potential ~500 mV and even below 300 mV, by using In-Situ Raman spectroscopy analysis [34]. Ishikawa et al. demonstrated that it is possible to intercalate Li^+-ion in the graphite anode without any additives. By

Table 1 Viscosity and ionic conductivity of the used electrolyte

Electrolyte	No salt addition		With adding 0.7 M LiFSI	
	Viscosity at 20 °C (mPa s)	Conductivity at 20 °C (mS/cm)	Viscosity at 20 °C (mPa s)	Conductivity at 20 °C (mS/cm)
EC-DEC (3:7)	7.68	7.24	–	–
EMI[FSI]	19	17.74	25.5	11.3
Py13[FSI]	39	9.14	52.1	5.8

using an appropriate anion like bis(fluorosulfonyl)imide (FSI) [35], we have confirmed this result [36]. We have found that with the same IL-cations by changing from TFSI to FSI anion the electrochemical properties can be vastly improved. To understand the FSI-anion effect on the graphite intercalation, recently some work was done on XPS characterization and it revealed that the surface layer on the graphite in both systems, EMI-TFSI and EMI-FSI, are chemically similar. This effect is still not well understood; we think further work should be addressed to this point. From the safety aspect, in our previous work [37], we found that the reactivity of some ionic liquids is higher than others; ILs with EMI cations are worse from safety point of view than those with BMMI, Py13, PP14, and TMBA. In order to work on a future battery we tried to combine the safe materials.

Following our previous work mainly on the anode, briefly recapitulated below, we have investigated here the $LiFePO_4$ cathode side, and, then the full Li-ion battery with an ionic liquid. Thus we present work here on a safe battery configuration containing carbon anode and $LiFePO_4$ cathode, and, Py13-FSI with LiFSI as salt additive plus gel polymer together constituting the electrolyte. Some effects of the polymer addition to the battery system are also examined.

Experimental

The solvents chosen for this work are two ionic liquids; 1-ethyl-3-methylimidazolium-bis(fluorsulfonyl)imide (EMI-FSI), *N*-methyl-*N*-propylpyrrolidinium-bis(fluorsulfonyl) imide (Py13-FSI) based on FSI anion (Fig. 1), produced by Dai-Ichi Kogyo, Seiyaku Co., Ltd, Japan (DKS). These ionic liquids (IL) contain less than 10 ppm (*w*/*w*) of moisture and less than 2 ppm (w/w) of halide and alkali metal-ion impurities. Our interest in these ILs is related to the FSI anion when combined with high conductivity and lower viscosity cations such EMI; also on the use of wider potential window IL (Py13). Two organic electrolytes were also evaluated; the standard electrolyte ethylene carbonate/diethylcarbonate EC/DEC–1 M $LiPF_6$ (UB, Japan) was used as the reference. The second organic electrolyte was EC-DEC, in which we have dissolved 1 M of lithium bis (fluorosulfonyl)imide (LiFSI) (from DKS, Japan) was used.

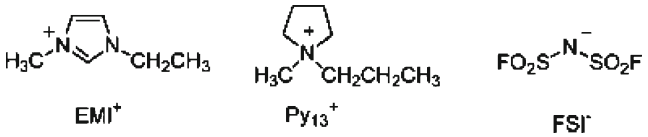

Fig. 1 Chemical structures of cations and anion of IL used in this study

A stainless-steel coin type cell was used for this study. The anode was a composite electrode containing 5 wt.% of PVDF (Kureha, Japan), 93% of natural graphite (Hydro-Québec) and very small amount of VGCF (vapor-growth carbon fiber) fiber (Showa-Denko, Japan). The cathode was constituted by 12% PVDF (Kruha, Japan), 82% of $LiFePO_4$ (Phostech-lithium, Canada) carbon coated, 3 wt.% of carbon black and very small amount of VGCF. We wanted to get the highest salt concentration but without going as high as it will cause some ion-pair formation and, thus, lower mobility and, thence, lower conductivity. Based on this, the electrolyte was prepared by adding 0.7 M LiFSI in both Py13-FSI, and, EMI-FSI ionic liquids. For the cell assembly, the Cellgard (3501) was soaked into the organic solvent or the ionic liquid electrolyte, under vacuum at 60 °C. The active surface area was 2 cm^2. The cell fabrication was performed in the glove box with lithium metal as the counter electrode. The electrochemical measurements were performed by using VMP-cycler (Biologic, France). The first formation cycles were obtained at constant charge–discharge at C/24. The electrodes were evaluated for power performance with the C-rate test, by varying the discharge current from C/12 to 40 C. The conductivity measurements were done by using a model CM-30R conductivity meter (from DKK-TOA Corp. Japan). The viscosity was measured by means of a MCR-30 viscometer (Anton-Paar, USA). Owing to its better safety profile, Py13(FSI) was considered for further study in this work.

The effect of gel polymer media was investigated with Py13(FSI) ionic liquid. The gel polymer was prepared by mixing of 5 wt.% of polymer with Py13(FSI) −0.7 M LiFSI and 1,000 ppm of thermal initiator perkadox (Akzo Nobel, USA). The polymer used was made from an ether-based low-molecular-weight cross-linkable polymer precursor (TA210, Daiichi Kogyo Seiyaku, Japan). The chemical formula has tri-function of poly (alkylene oxide) main chain with acrylate chain ends. This polymer has demonstrated a good electrochemical stability and high compatibility with high voltage cathodes like $LiCoO_2$ [38]. The electrodes were immersed in the mixture (polymer+IL+ initiator) and then heated at 60 °C under vacuum, a step necessary to help the (polymer+IL) electrolyte to penetrate in the pores deeply across the electrode thickness.

Then the cell was heated at 60 °C for 1 h in order to form the gel polymer. In-situ spectroscopy impedance was used to follow the resistance characteristics of the $LiFePO_4$ interface at different states of discharge.

Up till now, $LiCoO_2$ has been the main cathode material used in Li-Ion batteries, owing to its high energy density. However, the questionable long-term supply of cobalt material and its high cost present an uncertain future. So an alternative cathode material that is Co-free is urgently

Table 2 The first electrochemical characteristics of the graphite anode

Electrolyte	First discharge (mAh/g)	CE1 (%)	Reversible capacity (mAh/g)	CE2 (%)
EC-DEC–1 M $LiPF_6$	398	92.7	365	100
EC-DEC–1 M LiFSI	382	93.0	369	100
Py13-FSI+0.7 M LiFSI	468	80	367	98.3
EMI-FSI+0.7 M LiFSI	432	80.5	362	97.6

needed to prepare for the future applications of Li-ion battery technology in HEVs and PHEVs. Since the demonstration of $LiFePO_4$ by Padhi et al. [39, 40] as a potential cathode material, considerable interest has been generated due to its safety, low cost and environmentally friendly nature [41–47]. Furthermore, side reactions are minimized because of its flat voltage profile at 3.4 V vs. Li/Li^+. However, some other parts of the battery can cause problems in the scaled-up configuration. In Li-ion batteries, we found that in general the nature of electrolyte materials can have a great impact on the safety of the battery. In order to improve the safety of the lithium batteries, electrolyte should have lower inflammability and lower reactivity than the conventional electrolytes. Room temperature ionic liquids have suitable properties as safe electrolytes for lithium batteries due to their non-volatility and non-inflammability [48]. On the anode side the natural graphite material was used to make lithium-ion cell.

Results and discussion

Summary of data without polymer addition

The viscosity and conductivity values were measured at 20 °C. Table 1 shows the viscosity and the ionic conductivity of the pure "solvents" without salt addition. The conventional organic electrolyte shows the lowest viscosity. The table shows the ionic liquid having lower viscosity shows the higher conductivity.

The conductivity and viscosity (Table 1) of the conventional electrolyte does not follow the expected trend because the organic solvent has covalent bonding and few ions (by auto-ionization) and hence low conductivity. The ionic liquids, on the other hand, are by definition full of ions, and therefore, have higher conductivity than the organic solvents. The conductivity decreased and the viscosity increased when 0.7 M salt is added, possibly due to some ion-pair formation. Thus, in order to not create high ion-pair interaction in the IL, we have limited the salt addition to 0.7 M only. In ionic liquids, since the added salt cannot have the possibility of stabilization of its ionic constituents by solvation, such ion–ion interaction (quasi ion pairs) is not unexpected.

Behavior of anodes and cathodes in ionic liquid electrolytes

Recently [36], we have evaluated the graphite anodes in various ionic liquid electrolytes without polymer and the first electrochemical characterization is recapitulated in Table 2. The solid electrolyte interphase (SEI) with IL is well formed on the graphite anode, with 80% of coulombic efficiency in the first cycle. The reversible capacity was stable at 1 C cycling and the highest value was obtained with Py13(FSI) at 360 mAh/g. When $LiPF_6$ is replaced by LiFSI salt, the anode shows excellent performance with reversible capacity close to the theoretical capacity of 369 mAh/g and 93% coulombic efficiency in the first cycle. The LiFSI salt has a positive effect on the formation of coherent passive layer on the graphite. Further, the cell with FSI salt in EC/DEC has shown a stable SEI with good reversible capacity at 1 C rate, close to the theoretical value of 369 mAh/g.

The cell with IL based on EMI-FSI has shown 362 mAh/g as reversible capacity but only 80.5% coulombic efficiency. However, for the ionic liquid Py13, the reversible capacity was found close to the theoretical value of 367 mAh/g, while the first-coulombic efficiency was 80%. All these data explain well that LiFSI salt in FSI-based ionic liquid is suitable for use with the anode graphite, without any secondary reactions.

Similarly, the salient features of $LiFePO_4$ cathode in these electrolytes are encapsulated in Table 3 here. The impedance characteristics of these interfaces have been described in our recent paper [36]. The reversible capacity with EC/DEC-$LiPF_6$ was 158 mAh/g with 97.5% as coulombic efficiency in the first cycle (CE1). In curves of charge–discharge with LiFSI salt, the reversible capacity was quite comparable to EC-DEC-$LiPF_6$ electrolyte at 156.5 mAh/g, and 98% in the first cycle coulombic efficiency. With the ionic liquid Py13-FSI, a lower reversible capacity of 143 mAh/g was obtained with only 93% coulombic efficiency. However, with ionic liquid EMI (FSI), higher reversible capacity and coulombic efficiency, 160 mAh/g and 95%, respectively, were obtained.

Table 3 First electrochemical characteristics of the $LiFePO_4$ cathode

Electrolyte	First discharge (mAh/g)	CE1 (%)	Reversible capacity (mAh/g)	CE2 (%)
EC/DEC–1 M $LiPF_6$	158.2	97.5	158.0	98.0
EC/DEC–1 M LiFSI	156.5	98.0	156.5	98.0
Py13-FSI+0.7 M LiFSI	151.3	93.0	143.3	98.3
EMI-FSI+0.7 M LiFSI	164.0	95.0	160	97.0

During our study we noticed that the viscosity probably affects the performance of $LiFePO_4$ material due to the carbon coating on the surface of $LiFePO_4$ particles. When electrolyte has high viscosity as in an ionic liquid, the wettability of the carbon layer is more difficult due to its large surface area. Then the lithium-ions cannot migrate easily across this layer particularly in the first cycles. Moreover the viscosity can also prohibit the wettability of all the electrodes in depth, both anodes and cathodes because of the quasi tree-dimensional fractal nature of the electrodes, which contains not only meso-pores (easy accessible by the electrolyte) but also micro-pores which limit the electrolyte accessibility.

For impregnation and good contact of the electrolyte with the electrodes in high-viscosity systems such as the ionic liquids, a pretreatment in vacuum at 60 °C is necessary. On the cathode side, the reversible capacity was thus improved to 140 mAh/g at 1 C for Py13(FSI) by using vacuum treatment. The EMI(FSI) IL shows the highest value at 148 mAh/g, even higher than the reference electrolyte. Also, the rate capability has shown a small increase in the power performance until 2 C rate; however, above 2 C rate, high jump in the capacity was delivered from 40 to 80 mAh/g.

Thus, the LiFSI salt has good performance on both anode and cathode side. Also, we have shown that ionic liquid based on FSI as counter anion can be a good candidate for Li-ion battery [36]. However, for large configurations of Li-ion batteries for transportation, the safety aspect must be the first priority in the battery composition. Then, graphite/Py13(FSI)-LiFSI/$LiFePO_4$ seems to be the best choice in terms of safety and reversible capacity of the anode and the cathode. However, the power performance was found limited to 4 C rate which indicates that further improvement is thus needed. The polymer addition to the ionic liquid imparts the passivation layer; however with 5 wt.% of polymer the interface impedance is higher than with IL alone. The present work was undertaken to understand more fully the effect of polymer addition in the IL on the interface properties and the electrochemical performance for vapor pressure-free battery. For further tests we have selected the Py13(FSI) IL, based on its higher safety level as reported by Dahn et al. [37]. Using accelerated rate calorimetry the reactivity between some ILs and charged electrode materials (Li_1Si, $Li_7Ti_5O_{12}$ and $Li_{0.45}CoO_2$) was examined. In spite of the fact that most of the ILs alone show thermal stability higher than 250 °C–450 °C [37], when they are used in the cell at charged state, the thermal behavior is completely different. Some ILs have shown worse stability than conventional organic electrolytes. The ILs with EMI cations are worse in safety than those with BMMI, Py13, PP14, and TMBA. In other work Sakaebe et al. [49] have shown much improvement of the thermal stability of some ILs-TFSI achieved with LiTFSI additive, by using DSC. Mitsumoto et al. [50] have demonstrated by the charge/discharge cycling the stability of Li/Py13-FSI/$LiCoO_2$ cell, as compared to EMI and PP13 cations and to TFSI and FSI anions. They have found better cycling performance with Py13-FSI IL. Calorimetric study of Py13-FSI-based IL with LiTFSI salt additive, with charged and discharged graphite anodes has shown stable thermal behavior [51].

In-situ impedance spectroscopy of Li/IL/$LiFePO_4$ cells with and without polymer

1. Ionic liquid vs. conventional organic electrolyte

The in situ stepwise impedance spectroscopy was used to evaluate the Li/IL/$LiFePO_4$ cells at different states of discharge. The effect of polymer on the stability of the electrode interface was investigated with same cells by adding 1 or 5% by weight of the polymer. Figure 2 shows the first charge–discharge at C/24 curves and related impedance spectra of Li/$LiFePO_4$ of: (a) standard electrolyte (EC-DEC-$LiPF_6$), (b) IL (Py13(FSI)-LiFSI); the first-coulombic efficiency was found 97% and 100%, respectively. The reversible capacity was close to159 mAh/g for both cells.

The impedance spectroscopy measurements were taken at different states of charge of the cathode. A typical Nyquist plot of a Li/$LiFePO_4$ half cell is shown in Fig. 2. At high frequencies, the plot starts as a semicircle and, as the frequency decreases, it changes to a straight line. The semicircle reflects the impedance of the electrochemical reaction of the cell, while the straight line indicates diffusion of the electroactive species. The charge-transfer or the interface resistance (Ri) of the electrodes is determined by the two intersection points of the semicircle with the real axis. The diffusion resistance (Rd) is obtained from the difference between the total resistance (Rt) and the (ohmic+Ri) resistance.

Figure 3.a shows that the interface resistance (Ri), for the standard electrolyte, increases at 10% DoD (Depth of Discharge) then decreases with increase of the DoD till for fully delithiated $LiFePO_4$ it reaches 40 Ω. The highest value of Ri was 100 Ω, found at 10% DoD, when 10% of the lithium is removed from the $LiFePO_4$ structure. The cells having an ionic liquid as the electrolyte show that Ri increases at both low and high %DoD, contrary to the cell with standard electrolyte. After delithiation of $LiFePO_4$ up to 10%, the Ri increases from 150 Ω to 165 Ω, and then stays stable at around 150 Ω when more $LiFePO_4$ is transformed to $FePO_4$. When $LiFePO_4$ is completely transformed to the $FePO_4$, phase Ri decreased to lower values to finally reach 105 Ω. Since the high viscosity of the IL causes a problem of cathode wettability, compared to the

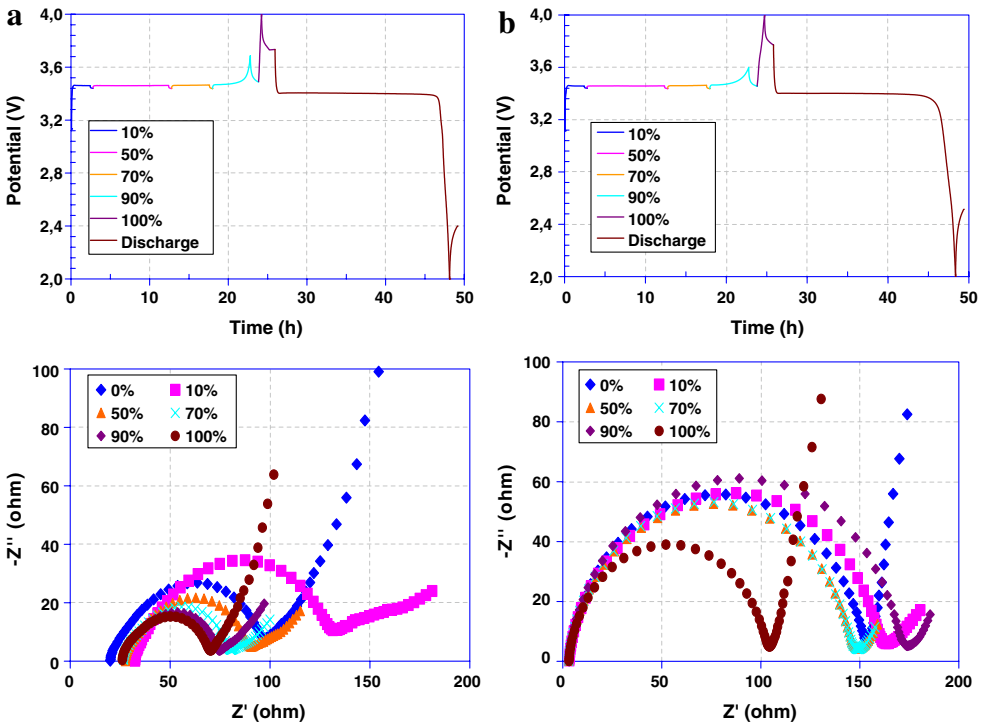

Fig. 2 Charge–discharge of the first cycle and impedance spectra of Li/$LiFePO_4$ cells; **a** EC-DEC–1 M $LiPF_6$ and **b** Py13(FSI)–0.7 M LiFSI electrolytes at different states of charge

conventional electrolyte, higher Ri is obtained with cells having IL as the electrolyte. Contrary to the conventional electrolyte, the average Ri behavior is maintained constant until 90% DoD after which an increase in Ri occurs. When all the iron phosphate material is delithiated and the monophase $FePO_4$ is the dominant phase, the Ri decreases to a level lower than the Ri of the fully lithiated monophase $LiFePO_4$ (0% DoD).

In the diffusion resistance part (Rd; Fig. 3b), Rd is higher in the conventional electrolyte than with the IL cell. Both electrolytes show a similar behavior; a decrease of Rd when the diphase $LiFePO_4$–$FePO_4$ coexists. Higher Rd was obtained with both monophase states of iron phosphate; $LiFePO_4$ at 0% DoD and $FePO_4$ at 100%DoD.

2. Ionic liquid with polymer additive

The effect of polymer addition to the IL was analyzed by in situ impedance spectroscopy. Figure 4 shows the charge–discharge of the first cycle and the associated impedance spectra at different states of charge of the Li/$FePO_4$ cells at (a) IL (Py13(FSI)-LiFSI), (b) IL+1% polymer and (c) IL+5% polymer; the first-coulombic efficiency was found to be 97%, 100%, 99%, respectively, with these cell configurations. The reversible capacity was close to159 mAh/g for all cells which is comparable to a cell with a standard electrolyte.

Figure 5a, shows the interface resistance Ri with IL cells, as well as for those to which 1% or 5% by weight of polymer is added. The Ri is increased when 5% polymer is added to the IL cell. However, when only 1% of polymer is added, Ri is lower than in the cell with IL alone at different level of %DoD. The average Ri values are maintained constant during the $LiFePO_4$–$FePO_4$ transformation with a higher Ri value at 90% DoD followed by lower Ri at monophase $FePO_4$. This behavior of the Ri variation is still present, independently of polymer addition. Therefore,

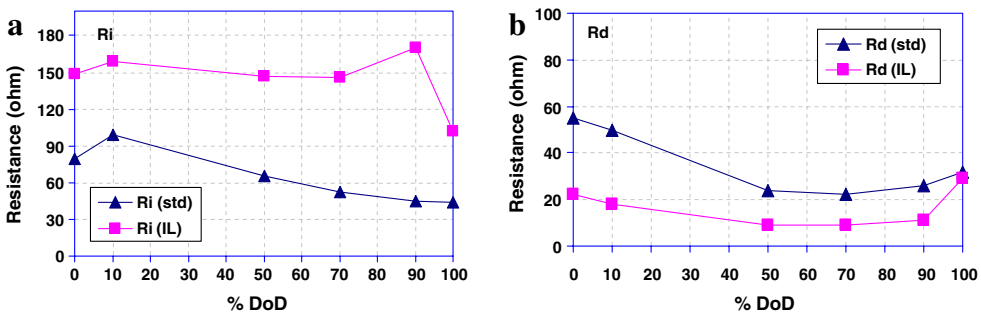

Fig. 3 Interface resistance "Ri" (**a**) and diffusion resistance "Rd" (**b**) of Li/$LiFePO_4$ cells with EC-DEC-1M $LiPF_6$ and Py13(FSI)–0.7 M LiFSI electrolytes as function of the state of charge

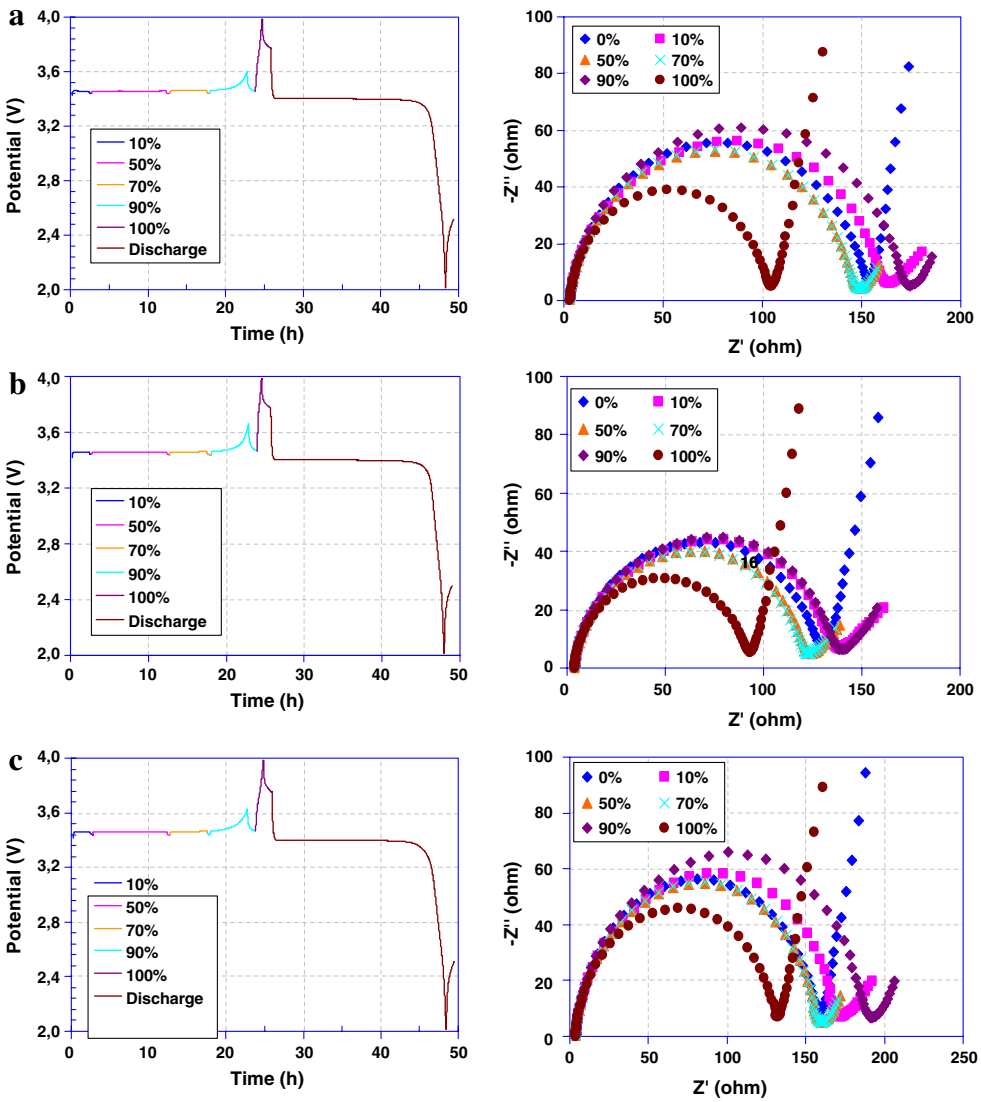

Fig. 4 Charge–discharge of the first cycle and impedance spectra of Li/$LiFePO_4$ cells with Py13(FSI)–0.7 M LiFSI; **a** 0% polymer, **b** 1% polymer **c** 5% polymer additive

from these results, we can assume that the addition of small amount of polymer (1%) improves the interface of the cathode in the cells with IL. This small amount of polymer can play an important role in making a stable solid electrolyte interphase layer (SEI), better than when the IL alone is used. The addition of more polymer in the IL cell (5%) shows a contrary effect with an increase of the interface resistance even higher than that for the IL without additive. We may infer that, the addition of 1% polymer stabilizes the SEI, and then reduces the interface resistance by forming a thin passivation film. Higher polymer content in the IL forms a thicker resistive layer which can lead to the increase in the Ri. The polymer would be expected to form a stable thin layer on both anode and cathode which is

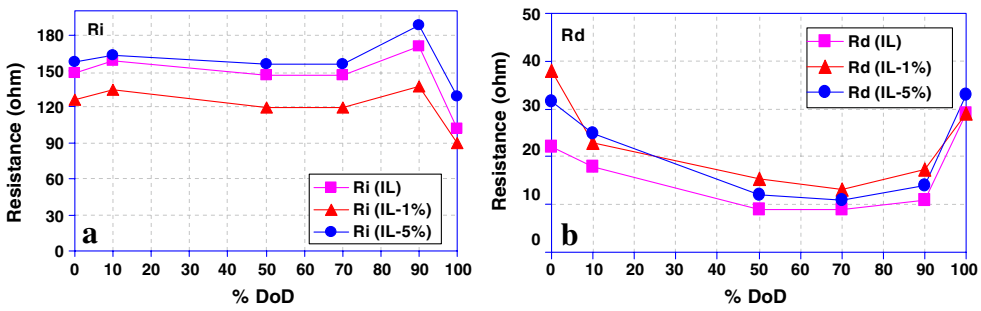

Fig. 5 Interface resistance "Ri" (**a**) and diffusion resistance "Rd" (**b**) of Li/$LiFePO_4$ cells with (IL+0%polymer), (IL+1% polymer) and (IL+5% polymer) as function of the state of charge

permeable to Li^+ ions. In the half cells, the polymer would passivate the lithium metal and decrease its reactivity, and reduce surface energy.

The diffusion resistance is plotted in Fig. 5b as a function of %DoD with different amounts of polymer in the IL. The same behavior of Rd may be noted at different states of charge with or without polymer additions. The highest value of Rd is obtained with the monophase iron phosphate; at 0% DoD with $LiFeO_4$ and at 100% DoD with $FePO_4$ phase. The diffusion process is easier when the diphase $LiFePO_4$–$FePO_4$ coexists, and particularly in the range of 50–70% DoD.

In order to investigate whether there is further stabilization after cycling, cells were cycled at C/24 for three cycles. The impedance measurements were taken at fully delithiated state (100% DoD). Figure 6 shows the impedance curves of the cells: (a) standard electrolyte (EC-DEC-1M $LiPF_6$), (b) IL (Py13-FSI), (c) (IL+1% polymer) and (d) (IL+5% polymer). The stabilization can be reached for the standard electrolyte (Fig. 6a) after the first cycle at 100 Ω of the total resistance (Rt) compared to the IL cell, in which (Fig. 6b) the stabilization can be achieved only after three cycles with Rt=194 Ω its Ri=156 Ω (Fig. 6b) compared to the standard electrolyte (Fig. 6a) with Rt=105 Ω and Ri=37 Ω. When a small amount of polymer is added (1%), stabilization still reached at the third cycle but at lower Rt=163 Ω and Ri=124 Ω (Fig. 6c). The addition of higher polymer content (5%; Fig. 6d) shows that the interface is not well stabilized and the Rt is 200 Ω with 166 Ω associated with interface resistance. Also to be noticed is the fact that the initial ohmic resistance in Fig. 6 was found higher in the standard organic electrolyte with 23 Ω. This resistance may be attributed to the electrolyte and/or to the organic reaction film formed by interaction of organic electrolyte with the lithium metal electrode; in the presence of IL, however, this ohmic resistance becomes vanishingly small, as would be expected for these high-conducting media, which also have no tendency to form resistive films at the surface which, if anything, would be expected to be covered by a conducting ionic salt layer.

The cells were cycled at C/4 rate for a long cycle life aging (Fig. 7), the reversible capacity was found stable in all cases at 149, 152, and 148 mAh/g respectively for (a) IL, (b) (IL+1 wt.% polymer) and (c) (IL+5 wt.% polymer). The coulombic efficiency remains constant during the cycling life with 99.6% for all cells. However, we noted an abnormal behavior with 5% polymer cell. In the first 20 cycles, the capacity increases and the coulombic efficiency fluctuates before the cell reaches the stable condition. Moreover, this result confirms the stabilization of both electrode interfaces of $LiFePO_4$ and lithium electrodes with IL which probably suppresses the dendrite formation on the lithium metal. The rate capability of the cell, Li/(IL+5 wt.% polymer)/$LiFePO_4$, is shown in Fig. 8. The cell delivers the full capacity until around C/2 rate, and then the discharged capacity starts decreasing to reach 82% at 2 C. At 4 C rate, the capacity dropped sharply to 47% and continues dropping as the discharge rate is increased. This drop in

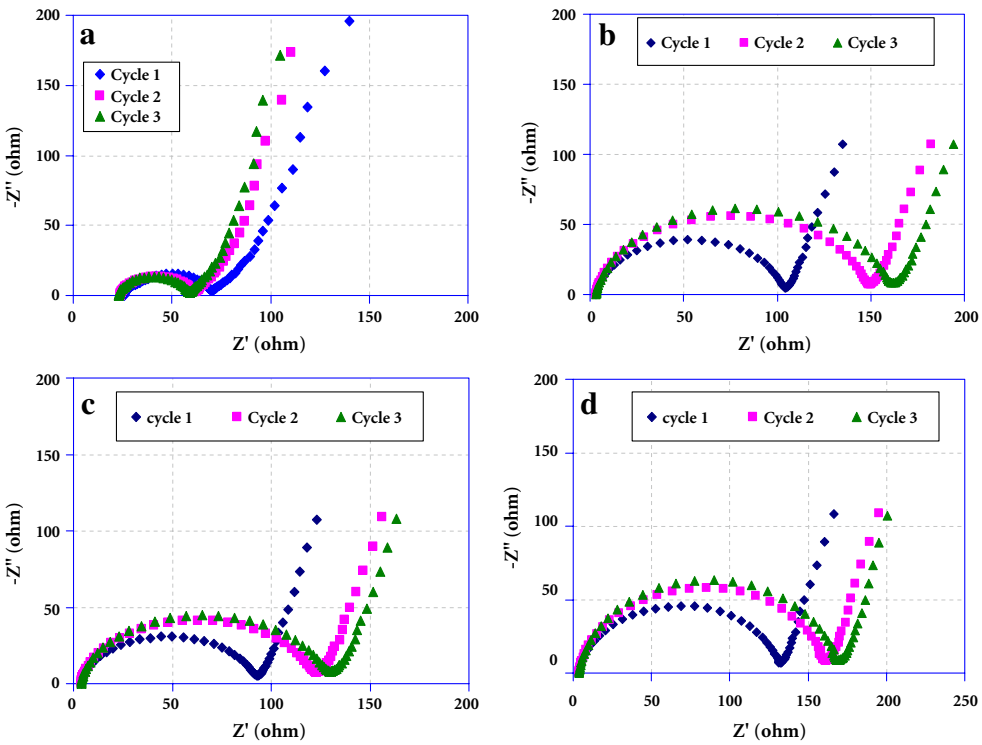

Fig. 6 Impedance curves of the Li/$LiFePO_4$ cells: **a** standard electrolyte (EC-DEC–1 M $LiPF_6$), **b** (IL+0%polymer), **c** (IL+1%polymer) and **d** (IL+5% polymer)

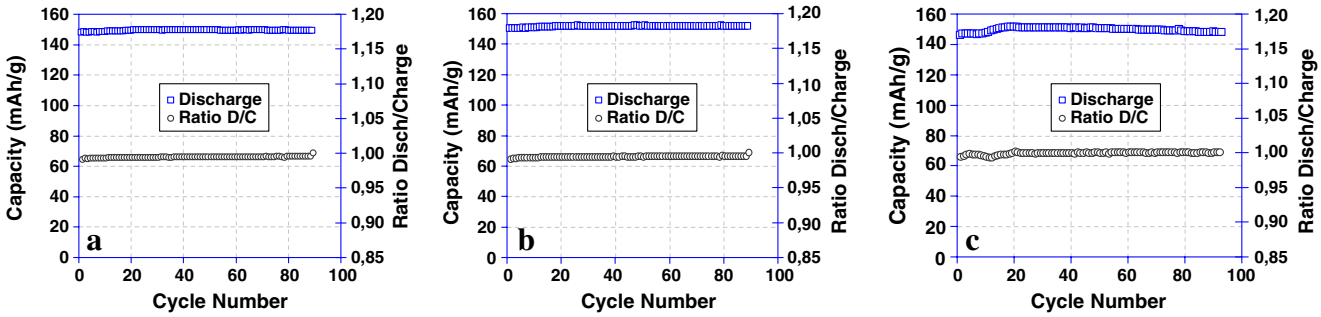

Fig. 7 Cycling behavior of Li/$LiFePO_4$ cells in different electrolytes

the capacity above 2 C rate perhaps indicates that the limiting process lies in the ionic liquid: it is well-known that a very high concentration of ions in the molten salt can lead to "over-population" of ions that can cause phenomena such as ion-pair formation and "salting out", in the sense that ion–ion distance is short thus disabling the "free" ion to make full contribution to the conduction [52, 53]. Such a situation, of course, does not exist in the standard organic electrolyte [36] in which the solvent molecules are abundantly available to solvate the lithium ions which then contribute to conduction.

Li-ion cell with IL and polymer gel

We have attempted to make full Li-ion battery with $LiFePO_4$ as cathode and graphite as the anode, by using Py13(FSI)-0.7MLiFSI as the electrolyte to which we have added 5 wt.% of polymer. Before making the Li-ion-cell, the graphite anode was also evaluated separately in a half cell with the same electrolyte composition (IL+5 wt.% polymer). Figure 9 shows the cycling behavior at C/4 of the graphite anode. In the first few cycles, a small fading of about 3% was noticed, and then the cell recovered with good reversible capacity stabilization at 342 mAh/g. Our choice for this amount of polymer is based on the safety aspect; the gel polymer cannot be well formed with lower than 5 wt.% of polymer in the IL-polymer mixture; hence, the desired electrode–gel interface aimed here can only be formed at polymer concentration of ≥5%. The cells have active surface area of 104 cm^2 (Fig. 10) and an installed capacity of 38 mAh. The first cycles of charge–discharge at C/24 show an increase in the coulombic efficiency (CE) from 68.4% in the first cycle to 96.5% in the third cycle (Fig. 11). The low first CE in Li-ion cell is more related to the graphite anode which has in the first cycle only 80% CE. Thus, further improvements should be aimed at the graphite anode side. The reversible capacity was 113 mAh/g. After three cycles, the CE recovers to 96.5% but the battery still needs more cycles to be efficient. The power capability was evaluated for this IL-Li-ion battery based on the discharge capacity obtained at C/12. The charge was maintained at constant regime at C/6 and the discharge regime ranged from C/12 to 40 C. Stable capacity, independently of the discharge rates, was obtained below

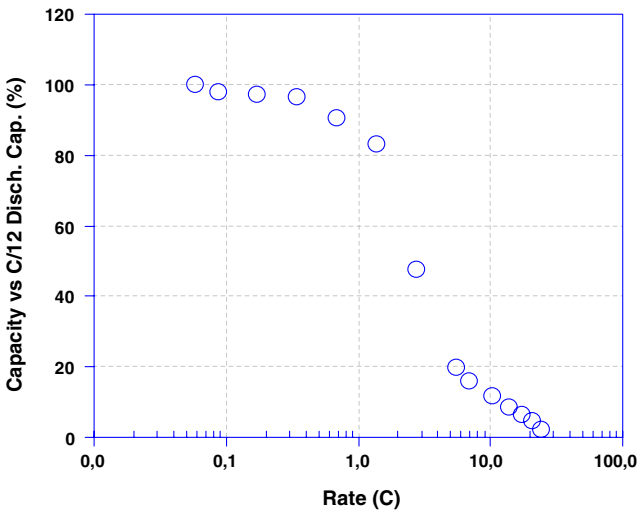

Fig. 8 Rate capability of Li-graphite cell with [Py13(FSI)–0.7 M LiFSI+5% polymer]

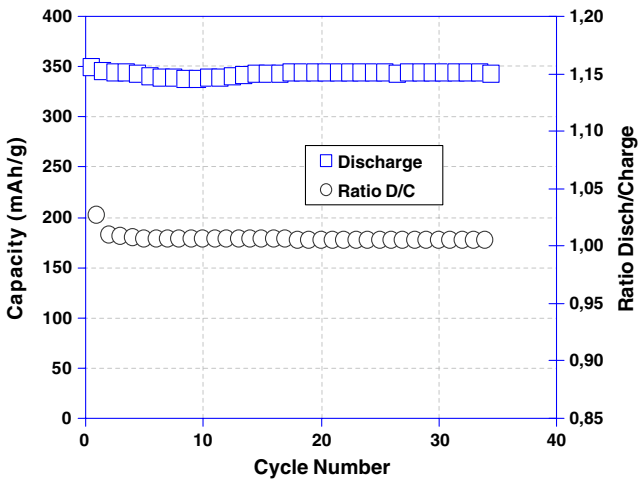

Fig. 9 Cycling behavior of Li-graphite cell with [Py13(FSI)–0.7 M LiFSI+5% polymer]

Fig. 10 Li-ion flat aluminum bag cell with an active surface area of 104 cm^2

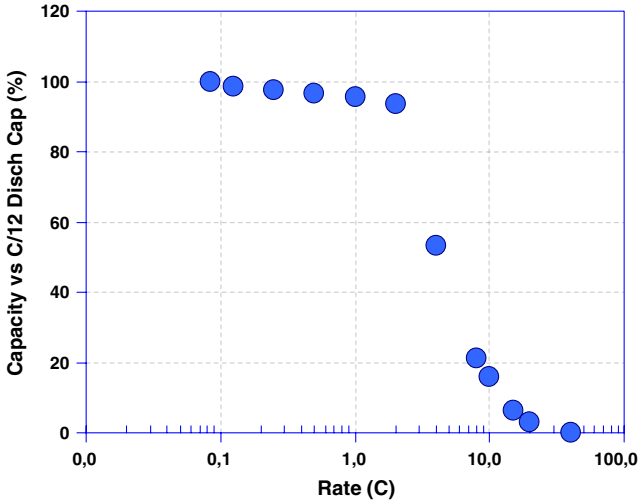

Fig. 12 Rate capability of Li-ion cell with [Py13(FSI)–0.7 M LiFSI+5% polymer]

and up to 2 C rate, as shown in Fig. 12. The capacity starts decreasing at rates above 2 C, with 54% of the rated capacity still delivered at 4 C. This limitation, as we have explained in the preceding paragraphs, arises from the high concentration of ions in IL, which induce a lower free pathway of ions in the media owing to ion pairing etc. [52, 53].

On the long cycling life, the cell was cycled at the C/4 rate between 4 V and 2 V. Figure 13 shows the behavior of the discharged capacity normalized to the initial discharged capacity as function of the cycle number. After 30 cycles, the capacity of the cell fades by 10%. This capacity fade, represented by 0.33% per cycle, is slightly higher than that in the Li-ion cell with standard electrolyte. Based on the cycling data of the separate half cells (Figs. 7 and 9) we cannot attribute this fading to any of the half cells; both electrodes separately have shown a good stability with Py13-FSI-polymer electrolyte. But when we assemble the full Li-ion cell, the source of lithium ions is limited, thus, the inefficiency of the graphite anode half cell (80%) consumes more lithium ion than standard electrolyte to form its SEI on the graphite anode. However, this SEI layer needs few cycles till it is fully stabilized. Hence, the balancing process between anode and cathode capacities in the IL media can be one of the problems causing capacity fading. The large active surface area of (104 cm^2) of the electrodes raises a technological difficulty related to the wettability of the whole active material of both electrodes with IL-polymer electrolyte. Notwithstanding this fact, we demonstrate that a Li-ion battery having $LiFePO_4$ and

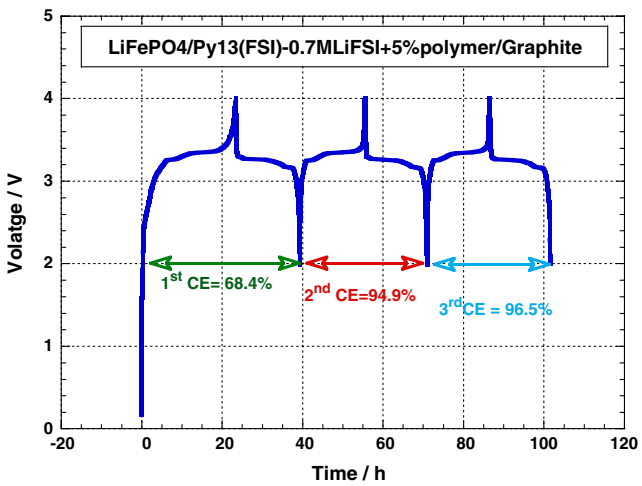

Fig. 11 The first charge/discharge cycles of Li-ion cell with [Py13(FSI)–0.7 M LiFSI+5% polymer]

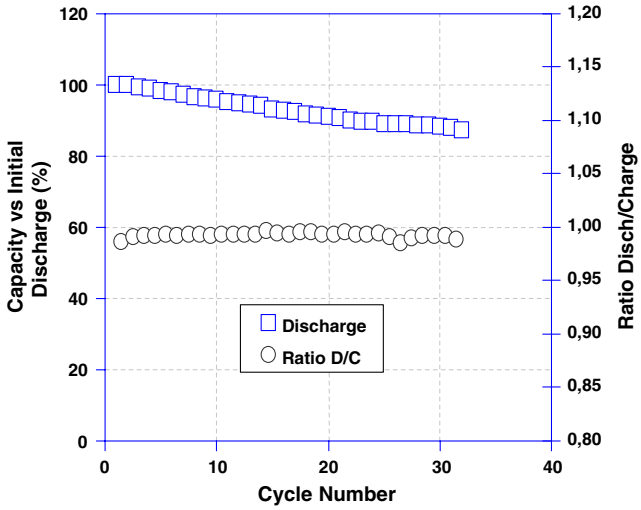

Fig. 13 Cycling behavior of Li-ion cell with [Py13(FSI)–0.7 M LiFSI+5% polymer]

graphite as the cathode and anode, respectively, with an ionic liquid as the electrolyte is achievable. Some applications where the high power is not the requirement can benefit from this technology. However, many technical parameters such as the electrode porosity, the separator porosity and the wetting process should be further improved during further technical development.

Conclusions

The in situ impedance spectroscopy was used to study the interface behavior of the $LiFePO_4$ cathode with IL and compared to the standard electrolyte. It was found that interfacial "Ri" decreased when $LiFePO_4$–$FePO_4$ phases coexist (90%>DoD>10%). On the other hand, the diffusion resistance "Rd" was found higher when the iron phosphate was present in the monophase state; $LiFePO_4$ (0% DoD) or $FePO_4$ (100% DoD).

When a small amount of polymer (1%) is mixed with IL, the interfacial resistance improves by forming a stable SEI at the electrodes. By increasing the polymer content at 5%, Ri and Rd increase, independently of the state of discharge. In all cases, Li-cells have shown a good cycling resulting from the stability of the permeable (to Li^+ ions) layer formed at the electrode surfaces. For the full Li-ion cell, a low first-coulombic efficiency was found at 68.4%, related to the low first CE of the graphite anode. The rate capability is good until 2 C rate, and above this rate the capacity drops to 54% of the rated capacity. This behavior is probably associated with the high population of ions causing some ion pairing [52, 53] which limits their freedom of mobility and prevents them from the full contribution to conduction in the battery. Further improvement should be focused to improve the CE of the anode side and technical optimization is needed; such as pores control in the electrodes and the separator, improving the wetting process in the electrodes, and the attainment of high rate performance before this technology is considered for commercialization.

Acknowledgment This work was financially supported by Hydro-Québec.

References

1. Tanaka T, Ohta K, Arai N (2001) J Power Sources 97–98:2. doi:10.1016/S0378-7753(01)00502-X
2. March RA, Vukson S, Sarampudi S, Ratnakumar BV, Smart MC, Manzo M et al (2001) J Power Sources 97–98:25–27. doi:10.1016/S0378-7753(01)00584-5
3. Takamura T (2002) Solid State Ion 152–153:19. doi:10.1016/S0167-2738(02)00325-9
4. Zaghib K, Charest P, Guerfi A, Shim J, Perrier M, Striebel K (2004) J Power Sources 134:124. doi:10.1016/j.jpowsour.2004.02.020
5. PNGV FreedomCar manual, T.Q. Duong. J Power Sources 89:244. doi:10.1016/S0378-7753(00)00439-0
6. Terada N, Yanagi T, Arai S, Yoshikawa M, Ohta K, Nakajima N et al (2001) J Power Sources 100:80–92. doi:10.1016/S0378-7753(01)00885-0
7. Nanis L, Bockris JO'M (1963) J Phys Chem 67:2865. doi:10.1021/j100806a519
8. Bockris JO'M, Richards SR (1965) J Phys Chem 69:671
9. Emi T, Bockris JO'M (1970) J Phys Chem 74:159. doi:10.1021/j100696a029
10. Fürth R (1941) Proc Camb Philos Soc 37:252
11. Huddleston JG, Willaur HD, Swatloski RP, Visser AE, Rogers RD (1998) Chem Commun (Camb) 1765. doi:10.1039/a803999b
12. Blanchard LA, Hancu D, Beckman EJ, Brennecke JF (1999) Nature 399:289. doi:10.1038/19887
13. Sato T, Masuda G, Takgi K (2004) Electrochim Acta 49:3603. doi:10.1016/j.electacta.2004.03.030
14. Kim YJ, Matsuzawa Y, Ozaki S, Park KC, Kim C, Endo M et al (2004) Soc 152:A710–A715
15. Xu J, Yang J, NuLi Y, Wang J, Zhang Z (2006) J Power Sources 160:621. doi:10.1016/j.jpowsour.2006.01.054
16. Garsia B, Lavalee S, Perron G, Michot C, Armand M (2004) Electrochim Acta 49:4583–4588. doi:10.1016/j.electacta.2004.04.041
17. Sakaebe H, Matsumoto H (2003) Electrochem Commun 5:594–598. doi:10.1016/S1388-2481(03)00137-1
18. Sakaebe H, Matsumoto H, Tatsumi K (2005) J Power Sources 146:693–697. doi:10.1016/j.jpowsour.2005.03.071
19. Matsumoto H, Sakaebe H, Tatsumi K (2005) J Power Sources 146:45–50. doi:10.1016/j.jpowsour.2005.03.103
20. Seki S, Kobayashi Y, Miyashiro H, Ohno Y, Mita Y, Usami A, Terada N, Watanabe M (2005) Electrochem Solid-State Lett 8:A577–A578. doi:10.1149/1.2041330
21. Cooper EI, Angell CA (1986) Solid State Ion 18–19:570. doi:10.1016/0167-2738(86)90180-3
22. Emanuel WX, Cooper EI, Angell CA (2003) J Phys Chem 107:6170. doi:10.1021/jp0275894
23. Matsumoto H, Yanagida M, Tanimoto K, Nomura M, Kitagawa Y, Miyazaki Y (2000) Chem Lett 8:922. doi:10.1246/cl.2000.922
24. Matsumoto H, Kageyama H, Miyazaki Y (2001) Chem Lett 2:182. doi:10.1246/cl.2001.182
25. Matsumoto H, Kageyama H, Miyazaki Y (2002) Chem Commun (Camb) 1726. doi:10.1039/b204046h
26. Seki S, Ohno Y, Miyashiro H, Kobayashi Y, Usami A, Mita Y et al (2008) J Electrochem Soc 155(6):A421. doi:10.1149/1.2899014
27. Sato T, Masuda G, Takagi K (2004) Electrochim Acta 49:3603. doi:10.1016/j.electacta.2004.03.030
28. Makino S, Sugimoto W, Takasu Y 214 ECS Meeting 2008] Abst # 531.
29. Holzpfel M, Jost C, Novak Chem P (2004) Commun 4:2098
30. Holzpfel M, Jost C, Prodi-Schaw A, Krumeich F, Wursig A, Buqa H et al (2005) Carbon 43:1488. doi:10.1016/j.carbon.2005.01.030
31. Sato T, Maruo T, Marukane S, Takagi K (2004) J Power Sources 138:253. doi:10.1016/j.jpowsour.2004.06.027
32. Baranchugov V, Markevich E, Pollak E, Salitra G, Aurbach D (2007) Electrochem Commun 9:796–800. doi:10.1016/j.elecom.2006.11.014
33. Kobayashi Y, Duchesne S, Dontigny M, Seki S, Mita Y, Miyashiro H, Charest P, Guerfi A, Zaghib K (2007) 211th ECS Meetting. Abst # 287
34. Markevich E, Baranchugov V, Salitra G, Aurbach D, Schmidt MA (2008) J Electrochem Soc 155:A132–A137. doi:10.1149/1.2811897

35. Ishikawa M, Sugimoto T, Kikuta M, Ishiko E, Kono M (2006) J Power Sources 162:658. doi:10.1016/j.jpowsour.2006.02.077
36. Guerfi A, Duchesne S, Kobayashi Y, Vijh A, Zaghib K (2008) J Power Sources 175:866. doi:10.1016/j.jpowsour.2007.09.030
37. Wang Y, Zaghib K, Guerfi A, Bazito FFC, Torresi RM, Dahn JR (2007) Electrochim Acta 52:6346. doi:10.1016/j.electacta.2007.04.067
38. Kono M, Nishiura M, Ishiko E (1999) J Power Sources 81–82:748. doi:10.1016/S0378-7753(99)00147-0
39. Padhi AK, Nanjundaswany KS, Goodenough JB (1997) J Electrochem Soc 144:1188. doi:10.1149/1.1837571
40. Padhi AK, Nanjundaswany KS, Masquelier C, Okada S, Goodenough JB (1997) J Electrochem Soc 144:1609. doi:10.1149/1.1837649
41. Striebel K, Guerfi A, Shim J, Armand M, Gauthier M, Zaghib K (2003) J Power Sources 119–121:951. doi:10.1016/S0378-7753(03)00295-7
42. Nakamura T, Miwa Y, Tabuchi M, Yamada Y (2006) J Electrochem Soc 153:A1108. doi:10.1149/1.2192732
43. Yu DYW, Donoue K, Inoue T, Fujimoto M, Fujitani S (2006) J Electrochem Soc 153:A835. doi:10.1149/1.2179199
44. Zaghib K, Striebel K, Guerfi A, Shim J, Armand M, Gauthier M (2004) Electrochim Acta 50:263. doi:10.1016/j.electacta.2004.02.073
45. Takahashi M, Ohtsuka H, Akuto K, Sakurai Y (2005) J Electrochem Soc 152:A899. doi:10.1149/1.1874693
46. Striebel K, Shim J, Strinivasan V, Newman J (2005) J Electrochem Soc 152:A664. doi:10.1149/1.1862477
47. Zaghib K, Julien CM (2005) J Power Sources 142:279. doi:10.1016/j.jpowsour.2004.09.042
48. Sakaebe H, Matsuumoto H (2005) In: Ohno H (ed) Electrochemical aspects of ionic liquids. Wiley, Hoboken, NJ, pp 173–186
49. Sakaebi H, Matsumoto H, Tatsumi K (2007) The 48th battery Symposium in Japan, November 13–15. 168
50. Matsumoto H, Sakaebe H, Tatsumi K, Kikuta M, Ishiko E, Kono M (2006) J Power Sources 160:1308. doi:10.1016/j.jpowsour.2006.02.018
51. Seki S, Kobayashi Y, Ohno Y, Miyashiro H, Mita Y, Terada N et al (2007) The 48th battery Symposium in Japan, November 13–15. 174
52. Bockris JOM, Reddy AKN (1970) Modern electrochemistry, vol 1. Plenum, New York
53. Hunt PA, Gould IR, Kirchner B (2007) Aust J Chem 60:9. doi:10.1071/CH06301